Supplemental Materials

Supplemental Table I: Reagents used in this study			
Reagent	Description	Details	Source
Plasmids			
Bacterial expression	pTrc-His_6-FAP-A	FAP WT	Ratliff Lab
	pTrc-His_6-FAP-$A^{\Delta 213-216}$	FAP lacking FBN-binding site	
Mammalian expression	pEGFP-$Rab5^{Q79L}$	Constitutively active Rab5	This Study
	pEGFP-Clathrin Light Chain		GA Rutter, U Bristol
	pEGFP-$Rab4^{S22N}$	Constitutively inactive Rab4	S. Caplan UNMC
	pEGFP-$Rab11a^{S25N}$	Constitutively inactive Rab11	
	pSRa HA-$Arf6^{T22N}$	Constitutively inactive Arf6	P. Chavrier, Institut Curie
siRNAs			
	anti-Human Clathrin Heavy Chain	sc-35067	Santa Cruz
	anti-Human Caveolin1	ON-TARGETplus L-003467	Dharmacon
Antibodies (Ab)			
Primary Ab	Mouse monoclonal anti-His_6	631212	Clontech
	Rabbit monoclonal anti-Fibronectin	F14	Epitomics
	Rat monoclonal anti-active β1 Integrin	9EG7	BD Pharmingen
	Rabbit polyclonal anti-FAP		Ratliff Lab
	Rabbit polyclonal anti-HA	HA.11	Covance
	Rabbit polyclonal anti-Caveolin1		BD Transduction
	Mouse monoclonal anti-Clathrin HC	X22	Affinity Bioreagents
	Mouse monoclonal anti-tubulin	DM1A	Abcam
	Mouse monoclonal anti-Lamp2	H4B4	Santa cruz
Secondary Ab	Goat anti-Mouse AlexaFluor-546		Molecular Probes
	Chicken anti-Rabbit AlexaFluor-647		
	Goat anti-Rabbit Cy2		Jackson Labs
	Goat anti-Rat Cy3		
Other			
	AlexaFluor647 maleimide		Invitrogen
	CF^{TM}-633 succinimidyl ester		Biotium
	Ni^{2+}:trisNTA-AlexaFluor-647	His_6-labeling reagent	This Study, see synthesis below
	DSPE- CF^{TM}-633	Fluorescent lipid for liposome preparation	

Supplemental Methods

Recycling experiments

A) Direct measurement of recycling: This experimental approach is designed to measure a putative decrease in the pool of internalized His_6-FAP as a function of time due to recycling. T24 cells were treated with leupeptin and bound to His_6-FAP as described in Materials and Methods. Then His_6-FAP was fluorescently labeled with 25µM Ni^{2+}:trisNTA-AlexaFluor-647 and clustered with 1/1000 anti-FAP antibodies as described for the endocytosis experiments. After 3h of internalization at 37°C in the presence of serum-free DMEM and 100µg/mL leupeptin, non-internalized surface probes (both Ni^{2+}:trisNTA-AlexaFluor647 and anti-FAP) were removed by rinsing cells with pH 2.0 buffer supplemented with 20mM EDTA for 60s. After washing, cells were allowed to recycle internalized His_6-FAP for up to 1.5h before removing putative recycled FAP and fixing. Internalized FAP and the lysosomal marker Lamp2 were investigated by immunofluorescence with specific antibodies.

B) Inhibition of recycling. This approach aims to detect accumulation of internalized FAP upon inhibition of recycling and lysosomal degradation. In T24 cells treated with 100µg/mL leupeptin, recycling was impaired by overexpressing constitutively inactive Rab4 and Rab11 constructs.

Organic synthesis methods

All reagents were obtained from commercial suppliers and used without further purification. All reactions (Supplemental Fig. 3 and 4) were carried out under a blanket of N_2 gas. Reaction progress was monitored by thin-layer chromatography (TLC) analysis. TLC spots were visualized by UV light (254nm) exposure. CH_3CN was distilled from CaH_2. Flash column chromatography was carried out using 230-400 mesh silica gel and analytical grade solvents. ^1H

and ^{13}C nuclear magnetic resonance (NMR) spectra were recorded with a Varian INOVA (300MHz) spectrometer. Chemical shifts are reported in ppm relative to the residual solvent peaks as internal standard. Peak multiplicities in ^{1}H NMR spectra are abbreviated as s (singlet), d (doublet), t (triplet), dd (doublet of doublet), m (multiplet), and br (broad). Mass spectrometry was performed by the MCMP Mass Spectrometry Service of Purdue University.

Di-t-butyl 2,2'-((6-(((benzyloxy)carbonyl)amino)-1-(t-butoxy)-1-oxohexan-2-yl)azanediyl)diacetate (**3**). $HClO_4$ (3.01 mL) was slowly added to a stirred solution of Z-Lys **1** (6.5 g, 23.18 mmol) in *t*-butyl acetate (80 mL). The mixture was stirred at 22 °C for 14 h before sequential extraction with H_2O (150 mL) and 0.5N HCl solution (150 mL). The combined aqueous solutions were treated with 10 % K_2CO_3 to give a solution of pH 9; the basic solution was then extracted with CH_2Cl_2 (3 × 100 mL). The combined organic layers were dried over anhydrous $MgSO_4$, filtered, and then concentrated to give **2** as a colorless oil. The oil was dissolved in CH_3CN (150 mL) before addition of $NaHCO_3$ (4.29 g, 51.07 mmol) and *t*-butyl bromoacetate (13.58 g, 69.64 mmol). The mixture was heated at reflux for 15 h, then cooled to 22 °C before concentration of the mixture under reduced pressure and extraction of the residue with ethyl acetate (2 × 150 mL). The combined organic layers were washed with saturated NaCl solution (2 × 100 mL), dried over anhydrous $MgSO_4$, and evaporated. The crude residue was purified by silica gel flash chromatography using 4:1 hexane:EtOAc as eluent to give compound **3** (11.62 g, 91%) as a colorless oil. ^{1}H NMR (300 MHz, $CDCl_3$) δ 7.30-7.35 (m, 5H), 5.08 (s, 2H), 3.44 (dd, J = 17.4, 11.1 Hz, 4H), 3.30 (t, J = 7.35 Hz, 1H), 3.20 (m, 2H), 1.62 (m, 2H), 1.53 (m, 4H), 1.45 (s, 9H), 1.43 (s, 18H); ^{13}C NMR (75 MHz, $CDCl_3$) δ 172.2, 171.2, 157.0, 137.34, 128.9, 128.6, 128.4, 81.64, 81.2, 66.9, 65.6, 54.4, 41.3, 30.6, 29.8, 28.7, 28.6, 23.5; HRMS

(ESI): $(M+H)^+$ *m/z* calc'd for $C_{30}H_{48}N_2O_8$ = 564.7107, found 565.0643. The NMR spectra are in agreement with previously published data.[1, 2]

Di-t-butyl 2,2'-((6-amino-1-(t-butoxy)-1-oxohexan-2-yl)azanediyl)diacetate (**4**). Compound **4** was synthesized according to a previously published procedure.[2]

2,2'-((5-(((Benzyloxy)carbonyl)amino)-1-carboxypentyl)azanediyl)diacetic acid (**5**). Compound **5** was synthesized according to a previously published procedure.[3]

Tetra-t-butyl 10-(4-(((benzyloxy)carbonyl)amino)butyl)-11-(2-((5-(bis(2-(t-butoxy)-2-oxoethyl)amino)-6-(t-butoxy)-6-oxohexyl)amino)-2-oxoethyl)-2,20-bis(2-(t-butoxy)-2-oxoethyl)-9,13-dioxo-2,8,11,14,20-pentaazahenicosane-1,3,19,21-tetracarboxylate (**6**). EDC (83 mg, 430 µmol) and HOBt (48 mg, 357 µmol) were added to a solution of **5** (40 mg, 110 µmol) in anhydrous DMF (8 mL) at 0 °C. After stirring the mixture for 15 min at 0 °C, a solution of **4** (148 mg, 487 µmol) and triethylamine (151µL, 1.1 mmol) was added at 0 °C and the mixture allowed to warm to 22 °C. After stirring the reaction at 22 °C for 24 h, the mixture was concentrated under reduced pressure and extracted with CH_2Cl_2 (2 x 15mL). The crude residue was purified by silica gel flash chromatography using 10:1 CH_2Cl_2:MeOH as eluent to give **7** (167 mg, 94%) as an oil.^{1}H NMR (300 MHz, $CDCl_3$) δ 7.34 (m, 5H), 5.08 (s, 2H), 3.45 (m, 16H), 3.19 - 3.31 (m, 12H), 1.65 (m, 8H), 1.53 (m, 16H), 1.46 (s, 27H), 1.44 (s, 54H); ^{13}C NMR (75 MHz, $CDCl_3$) δ 172.3, 171.5, 170.7, 162.6, 156.5, 136.8, 128.5, 127.981.1, 80.7, 66.4, 65.0, 56.2, 53.7, 40.6, 39.3, 31.4, 30.2, 29.9, 29.5, 29.3, 28.7, 28.2, 28.1, 23.4, 23.1; MS (positive

ESI): $(M+H)^+$ *m/z* calc'd for $C_{84}H_{144}N_8O_{23}$ = 1633.03, found 1633.90. The NMR spectra are in agreement with previously published data.[1]

Tetra-t-butyl 10-(4-aminobutyl)-11-(2-((5-(bis(2-(t-butoxy)-2-oxoethyl)amino)-6-(t-butoxy)-6-oxohexyl)amino)-2-oxoethyl)-2,20-bis(2-(t-butoxy)-2-oxoethyl)-9,13-dioxo-2,8,11,14,20-pentaazahenicosane-1,3,19,21-tetracarboxylate (**7**). Palladium on carbon (500 mg of 10 wt% Pd/C) was added to a solution of **6** (1.6 g, 979 µmol) in MeOH (30 mL). After stirring the reaction at 22 °C for 12 h under 1 atm H_2, the mixture was filtered and evaporated under reduced pressure to give **7** (1.5 g, 99 %). ^{1}H NMR (300 MHz, $CDCl_3$) δ 3.42 (m, 16H), 3.21 - 3.29 (m, 12H), 1.79 (m, 4H), 1.52 (m, 16H), 1.41 (s, 27H), 1.40 (s, 54H); ^{13}C NMR (75 MHz, $CDCl_3$) δ 172.4, 170.8, 81.2, 81.1, 65.2, 53.8, 39.2, 30.3, 29.0, 28.2, 28.1, 23.5, 23.3; MS (positive ESI): $(M+H)^+$ *m/z* calc'd for $C_{76}H_{138}N_8O_{21}$ = 1499.00, found 1499.95. The NMR spectra are in agreement with previously published data.[1]

Compound **8.** Compound **7** (1.5 mg, 1mmol) was added to a solution of AlexaFluor647 maleimide (1 mg, 800 µmol) and triethylamine (11 µL, 8 mmol) in DMF (5mL). After stirring the reaction at 22 °C for 5 h, the mixture was passed through a Sephadex G-15 column and the eluate lyophilized to give **8** (2 mg, 90%).

trisNTA-AlexaFluor647 (**9**). Compound **8** (2 mg, 727 µmol) was diluted in dichloromethane (1 mL) and trifluoroacetic acid (0.7 mL). The reaction mixture was stirred at 22 °C for 4 h before concentrating the solution under reduced pressure to give **9** (1.6 mg, 99%).

Ni^{2+}:trisNTA-AlexaFluor647 (**10**). $NiSO_4$ (100 µL of 50 mM stock solution, 2.139 mol) was added to Compound **9** (1.6 mg, 713 µmol) in H_2O (1.5 mL). The reaction mixture was stirred at 22 °C for 2 h before passing it through a Sephadex G-15 column. Lyophilization of the eluate gave **10** (1.6 mg, 99%). A 25µM stock solution of **10** was prepared for labeling His_6-FAP in subsequent cellular localization studies.

DSPE- CF™-633: DSPE was dissolved in dry CH_2Cl_2 and then transferred to 1 mL vial with CF™-633 succinimidyl ester. The mixture was placed on a shaker and mixed overnight before passing it through a lipophilic Sephadex LH-20 column that had been equilibrated with 10% MeOH in CH_2Cl_2. Column fractions were evaporated to dryness and then re-dissolved in 1mL of $CHCl_3$ for use in liposome formulations.

Supplemental References

1. Huang, Z. H.; Park, J. I.; Watson, D. S.; Hwang, P.; Szoka, F. C., Facile synthesis of multivalent nitrilotriacetic acid (NTA) and NTA conjugates for analytical and drug delivery applications. *Bioconjugate Chem.* **2006,** *17*, 1592-1600.

2. Hussein, W. M.; Ross, B. P.; Landsberg, M. J.; Levy, D.; Hankamer, B.; McGeary, R. P., Synthesis of Nickel-Chelating Fluorinated Lipids for Protein Monolayer Crystallizations. *J. Org. Chem.* **2009,** *74*, 1473-1479.

3. Altin, J. G.; Banwell, M. G.; Coghlan, P. A.; Easton, C. J.; Nairn, M. R.; Offermann, D. A., Synthesis of NTA(3)-DTDA - A chelator-lipid that promotes stable binding of His-tagged proteins to membranes. *Aust. J. Chem.* **2006,** *59*, 302-306.

Legends to supplemental figures.

Supplemental Fig. 1. The association of purified FAP with cell-bound Fibronectin is resistant to acidic and bladder instillation conditions. A. Following FAP binding, the cells were washed and incubated with 10ml of pH=4.8 buffer (0.2N Acetic Acid, 150mM NaCl) at room temperature for the indicated times, cells were fixed and immunostained with anti-His primary and anti-mouse AlexaFluor546 secondary antibodies. FAP fluorescence that remained associated with cells was quantified as described in Materials and Methods (AU: Arbitrary Units). **B-D**. Cell-associated FAP in the presence (**B** and **D**) or absence (**C**) of vesical instillation buffer and 50% urine (**D**) was detected using a Ni^{2+}: tris NTA-AlexaFluor647 probe. Arrows point to some areas of colocalization. Scale bar: 20microns

Supplemental Fig. 2. FAP internalization can be induced by sequential incubation with specific mouse monoclonal and anti-mouse IgG polyclonal antibodies. Cells were treated as in Fig. 2 except that they were sequentially incubated with primary and secondary antibodies at 10°C to induce FAP clustering. FAP-labeled cells were incubated with 1:1000 mouse monoclonal anti-His_6 antibody (α-His MAb) for 30min and then crosslinking was induced by addition of 1:2000 polyclonal Goat anti-mouse IgG AlexaFluor546 antibody (α-Mouse PAb) for 15min. Internalization was then allowed to progress for 3h at 37°C. Arrows point to some areas of colocalization. Scale bar: 20microns.

Supplemental Fig. 3. FACS analysis of FAP internalization and recycling. T24 cells were allowed to internalize FAP in the presence (+) and absence (-) of an anti-FAP antibody (α-FAP

Ab) as described in Materials and Methods. **A**. Example of Scatter plots obtained during this study. Percentage of cells containing high levels of intracellular FAP (included in the depicted gate) is indicated. Control values obtained in the presence of the Ni^{2+}:trisNTA fluorescent probe, but in the absence of either FAP or antibody-crosslinking are shown. **B**. Results are expressed as the ratio between gated cells (upper panel) and the ratio of median fluorescence intensity (FI—lower panel) in the presence and absence of α-FAP Ab (+Ab/-Ab). Although variation in-between experiments (e.g., percentages) was observed, ratio values were very reproducible. Statistical analysis was performed using the t-test (**: $p<0.05$). **C**. Following internalization leupeptin-treated T24 cells were stripped of non-internalized FAP and allowed to recycle for the indicated times. Putative changes in the amount of internalized FAP due to recycling were monitored as described in A and B.

Supplemental Fig. 4. **Effect of Clathrin or Cav-1 knock-down on the uptake of FAP and transferrin.** Cells were mock-treated or knock-down with specific siRNA pools and assayed for endocytosis of FAP and transferrin (Tf) as described in Material and Methods. Arrows point to some areas of colocalization. Scale bar: 10microns.

Supplemental Fig. 5. Synthesis route for the preparation of lysine NTA intermediate. See supplemental materials for details.

Supplemental Fig. 6. TrisNTA-AlexaFluor-647 synthesis pathway. See supplemental materials for details.

Supplemental Fig. 1

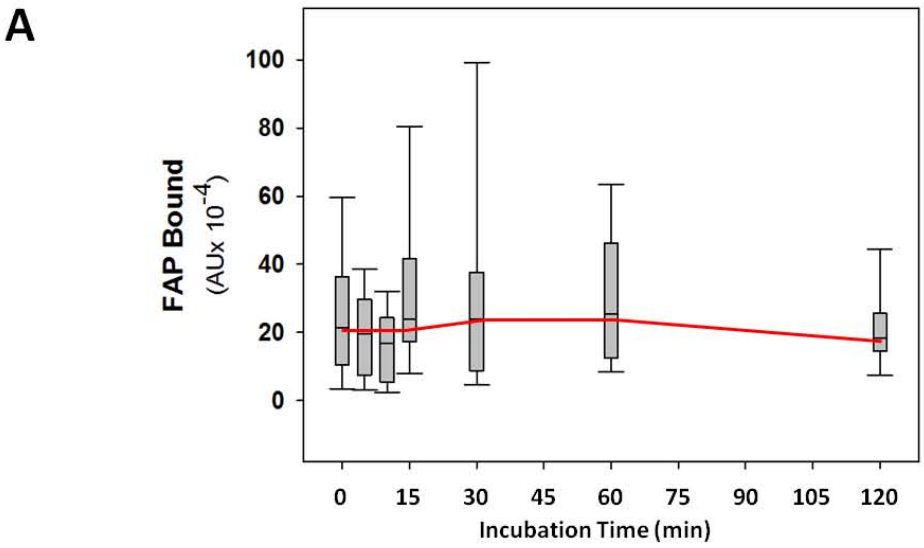

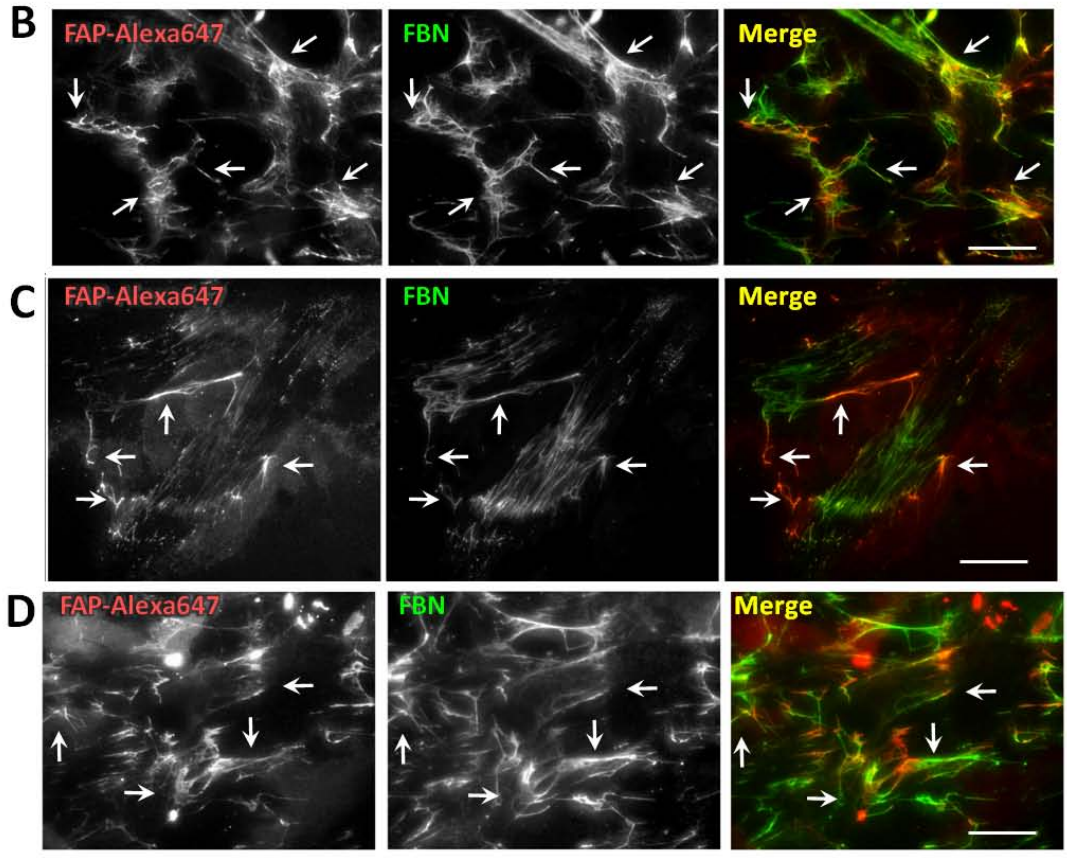

Supplemental Fig. 2

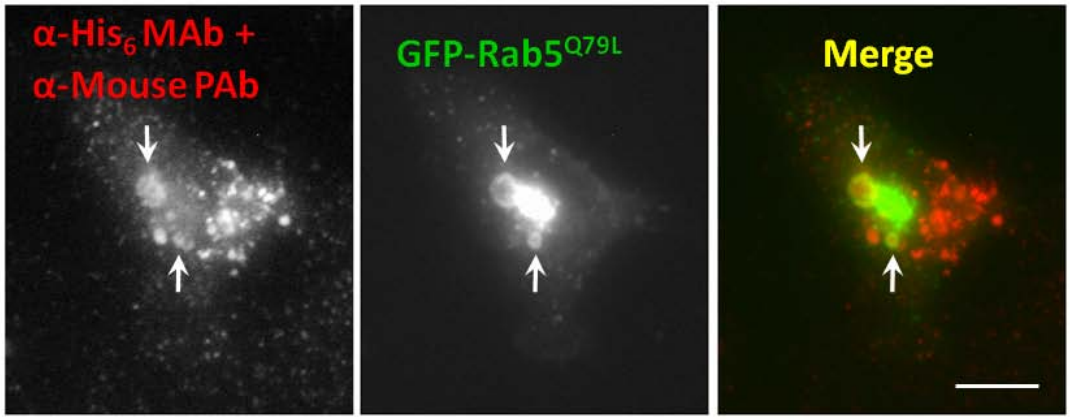

Supplemental Fig. 3

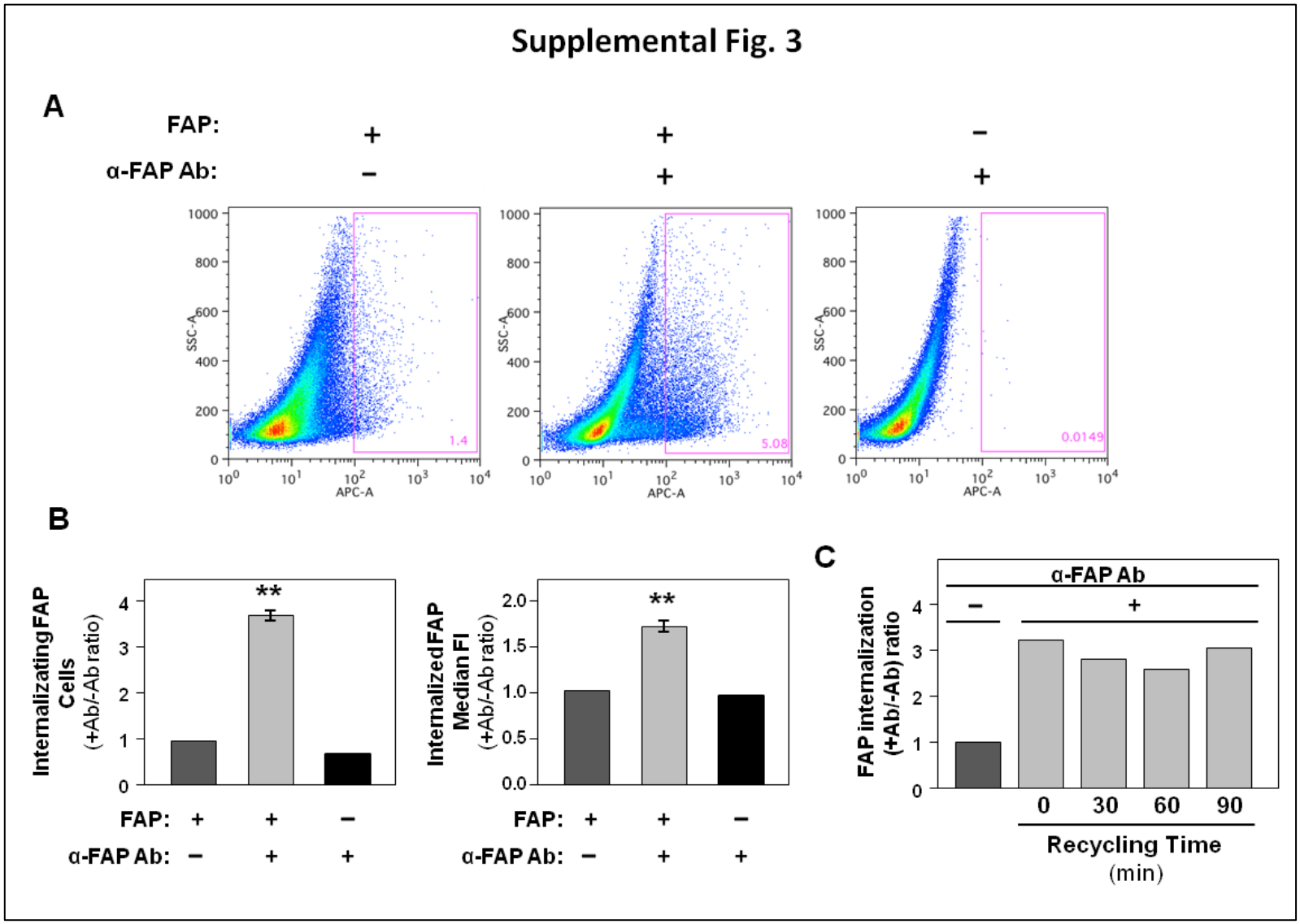

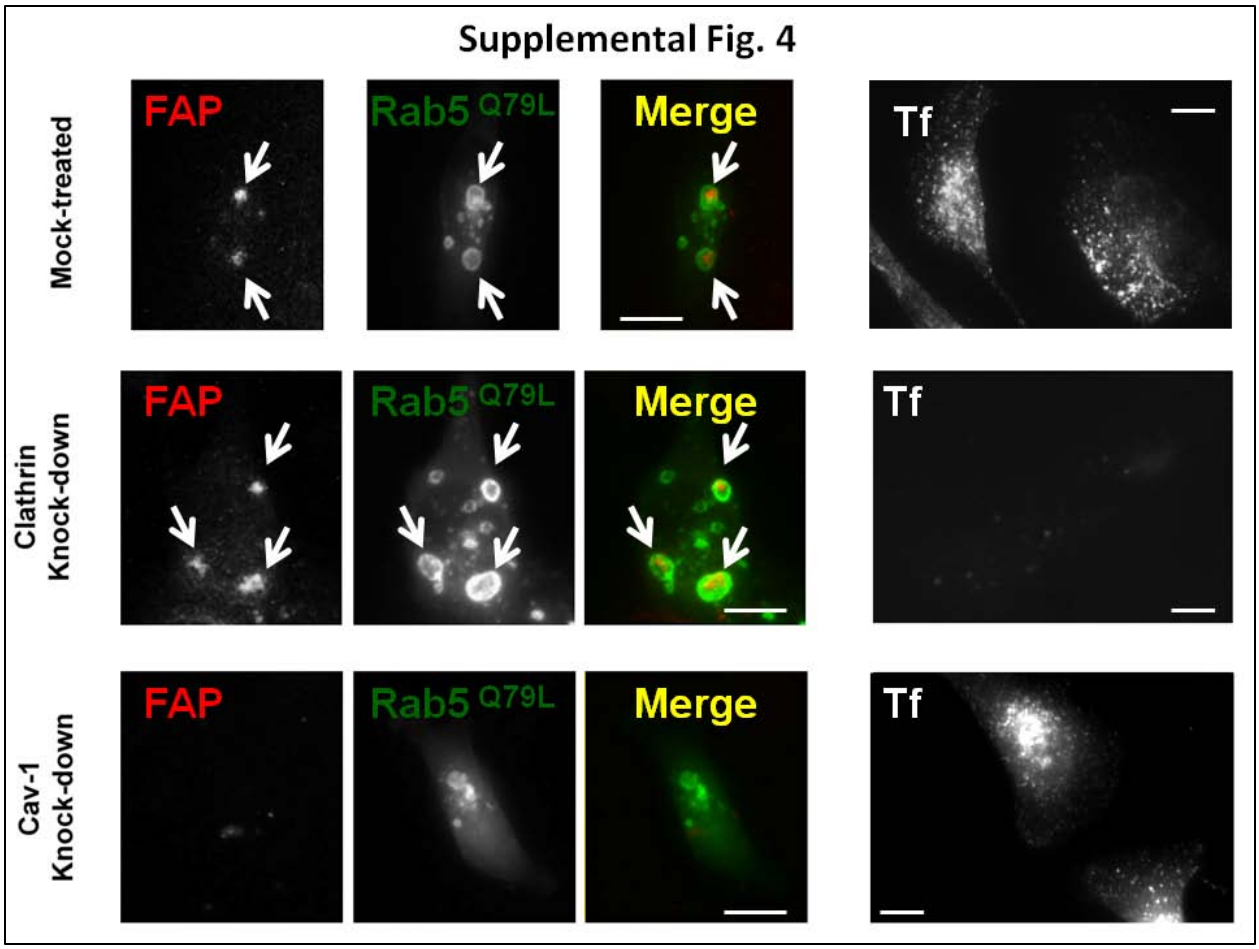
Supplemental Fig. 4
Mock-treated
Clathrin Knock-down
Cav-1 Knock-down
FAP
Rab5 Q79L
Merge
Tf

Supplemental Fig. 5

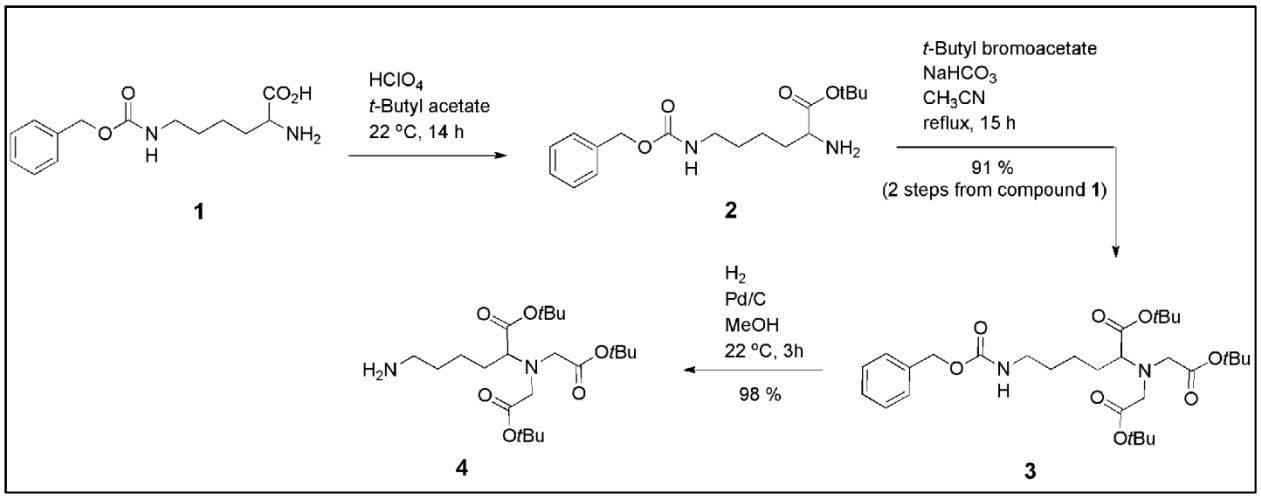

Supplemental Fig. 6